DEVELOPMENT OF A MICRO-FID USING A DIFFUSION FLAME

BY

JIHYUNG KIM

THESIS

Submitted in partial fulfillment of the requirements
for the degree of Master of Science in Mechanical Engineering
in the Graduate College of the
University of Illinois at Urbana-Champaign, 2011

Urbana, Illinois

Adviser:

Professor Mark A. Shannon

ABSTRACT

A micro-flame ionization detector (micro-FID) was developed operating with a diffusion flame with a folded flame structure. Unlike conventional FIDs, an air-hydrogen diffusion flame was developed and tested in an encapsulated structure of Quartz-Macor®-Quartz layers. Diffusion flames are generally known to be more controllable and stable than premixed flames, which fits our purpose for the micro-FID, where the stability plays an important role for many applications. Various Macor designs including a burner cavity and a micro-channel were tested to obtain highest output sensitivity over methane test samples. In order to gauge sensitivity of the device, collected electric charge per mole (C/mol) was calculated and taken as a reference value of ionization efficiency. The result was 1.959×10^{-2} C/mol for methane which was about 34 times higher compared to the result obtained using a counter-flow flame, which was 5.73×10^{-4} C/mol for methane, while one of the commercial macro FIDs has 10^{-1} C/mol. This result shows that the micro-FID using the folded flame structure enhances ionization with less leakage of the analytes than the classical counter-flow flame design.

ACKNOWLEDGMENTS

I would like to thank Prof. Mark A. Shannon for guiding and supporting my research with mentorship and encouragement throughout my studies at University of Illinois at Urbana-Champaign. Your passion in research and the love for your students inspired me in many ways. I am also grateful to Prof. Dimitrios C. Kyritisis for guiding me with the academic and research work. I deeply appreciate Dr. Kang, Dr. Bae, and Dr. Yeom for working together. I appreciate Dr. Mensing for teaching me how to organize my writing. I am lucky and feel grateful to have the opportunity to spend time together with members in Shannon research group. And most of all I want to thank my parents for their love and support.

TABLE OF CONTENTS

List of Tables

List of Figures

CHAPTER 1

INTRODUCTION

A Flame Ionization Detector (FID) can be used as a detector for hydrocarbons. The measurement is a results of the chemical ionization of hydrocarbons in an air-hydrogen or oxy-hydrogen flame. The hydrocarbons can be detected by measuring the resulting ion current. In the air-hydrogen flame or oxy-hydrogen flame, the injected organic compounds decompose into hydrocarbon radicals that react with oxygen and produce a large number of ions via reaction.

$$CH+O \rightarrow CHO^{+} + e^{-}$$

The CHO^{+} ion reacts quickly with water produced in the flame to produce hydroxonium ions (H_3O^{+}). This charge is the main species that is measured for the FID response[1].

$$CHO^{+} + H_2O \rightarrow H_3O^{+} + CO$$

The ions are collected by applying an electric field around the flame. Consequently the signal is proportional to the number of carbons inside the injected sample gas. Due to its sensitivity and detection limits of hydrocarbons, FID has been widely used in research and industry. FID has been extensively used in research and industry in tandem with gas chromatographs (GC) to analyze gas samples. An increasing interest in the miniaturization and portability has motivated the development of detectors compatible with GC devices.[2, 3] A portable micro-FID will be useful to the extent that it can be compared to a conventional FID. This micro-FID can potentially be used to identify chemical threats, spills, and for environmental monitoring in the field.

In conventional FIDs, micro-catalytic combustors are employed.[1, 4] The micro-combustor is made up of a catalytic film deposited on the surface of a micro-scale hot plate. Although catalytic combustion can sustain a flame with a relatively low fuel consumption rate at the micro-scale, the presence of catalysts affects the generation of ions from hydrocarbons, which will reduce the FID signal making those of catalytic combustion challenging in micro-FID. Kuipers and Müller *et al* [5] proposed a micro-FID using a premixed flame with oxygen and hydrogen. The oxy-hydrogen flame burns in a silicon channel which is encapsulated inside a glass-silicon-glass sandwich structure which was proposed by Zimmermann *et al.* [6, 7, 8]

1.1 Scope of the present work

In conventional FIDs, either a premixed or an open diffusion flame has been used. For pre-mixed flames the controllability of the fuel and oxidizer flow rate is limited due to the intrinsic flame speed. On the other hand, diffusion flames are known to be more controllable and stable than premixed flames. Hence, the current work will focus on the development of a micro-FID using an air-hydrogen diffusion flame.

As a first step to implement such a device, a stable flame with thickness below 1mm will be established. This thesis focuses on the design of the channel to create a stable and highly sensitive diffusion flame within the specified thickness. We start with the channel designs that can create a stable diffusion flame for a micro-FID. Various geometries of micro-channels are designed and tested in order to increase the sensitivity of the FID output. Increasing the sensitivity is attributed to an increase in the percentage of the ionization of the injected sample analytes. In other words, the channel is designed to create a flame that minimizes the loss of the sample analytes.

CHAPTER 2
EXPERIMENTAL SETUP

Initial experiments were performed in order to observe the flame in silicon channels with different shapes. In the early stages of the experiments, silicon channels were used in order to employ the benefit of fabricating various channels using a batch process. After determination of the optimal shape of the channels, Macor was machined instead of silicon for the channel structure in order to minimize the leakage current. A detailed description of the experimental apparatus involved and the fabrication process of the micro-FID components is provided in this chapter.

2.1. Flame visualization

As shown in Fig. 1, the micro-FID is composed of a silicon channel (750μm thickness), two sealing gaskets (high temperature resistance silicone), and two Quartz plates (25.4mm × 25.4mm × 1.5748mm, Technical Glass Products, Painesville, OH, U.S.). In the initial stages of the research the focuse was on the flame shape, and silicon was used to fabricate the channels. Using MEMS fabrication techniques allows various channel designs and more efficient comparisons of the different types of silicon channels. Two quartz plates were used to sandwich the silicon channel and make an encapsulated structure to enhance the stability of the diffusion flame.

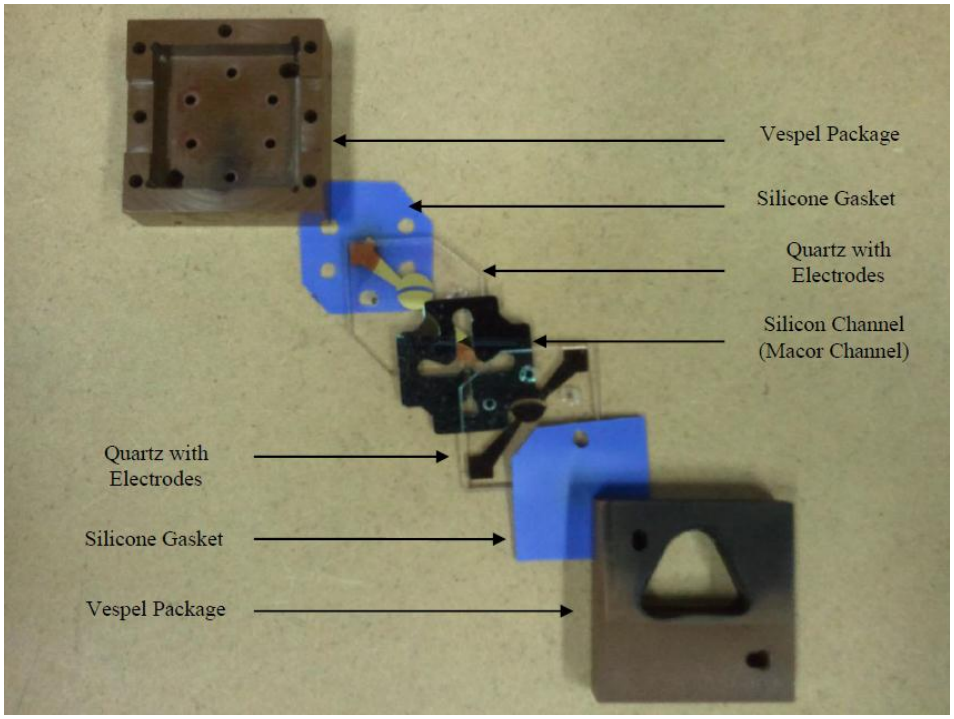

FIGURE 1. Micro-FID components including; silicon channel, two sealing gaskets, and two Quartz plates with patterned electrodes, which are assembled together in a Vespel package.

Flame structures with various channel geometries were visualized and investigated using an Andor 1-Star DH712 Intensified Charge-Coupled Device (ICCD) camera. Several silicon channels were designed and fabricated with different angles between the hydrogen and air channel. Channel designs with inlet gas angles from near 0º (air and H_2 coming from the same direction), to a counter-flow (Air coming from the top and hydrogen coming from the bottom) design were tested.

2.2. Signal Detection

During the evaluation of the micro-FID signals, a material called Macor was substituted for silicon to minimize the leakage current that was occurring between the silicon and quartz

plates. Macor is a machinable glass-ceramic. Here, Macor was chosen due to its high electric and thermal characteristics which can minimize the leakage current between the quartz and the fluidic channel. (>10^{16} ohm-cm and stable up to temperatures about 1000 °C).

The flame burns inside the Macor channel which was sandwiched between two quartz plates with patterned electrodes. Two pairs of Cr/Au electrodes are designed and fabricated on the quartz layers to establish the electric field collecting the ions. The top quartz plate contained the hole for the exhaust gas to exit while the bottom quartz plate had holes into which the hydrogen and air were separately supplied. The FID stack was packaged inside a Vespel package in order to minimize the leakage current and provide the connections for tubing to supply the gases.

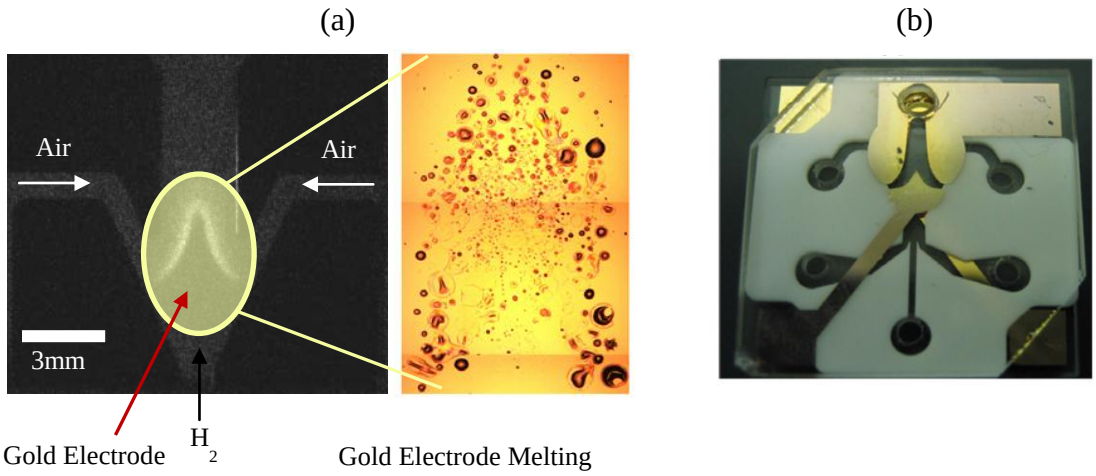

FIGURE 2. **(a)** The air-hydrogen flame is melting the electrodes, causing damage to the electrodes and unwanted noise signals.

(b) In order to avoid the flame area, the electrodes are split into two parts with a pattern matching the flame shape for the particular flame shape.

Figure 2a shows that the flame was captured inside the micro-fabricated silicon structure with the total thickness of 750μm. As shown in Fig.2 (a), the damaged area on an electrode due

to the high temperature can be localized along the flame. In order to locate the electrodes as close as possible to the flame without melting, the electrode was split in two parts as shown in Fig.2b.

The inlet gas was controlled using mass flow controllers (FMA 5400/5500 Omega, Stamford, CT, U.S.). Figure 3 shows the overall experimental setup for the signal detection. Air and hydrogen were supplied from the gas tank to the micro-FID. The injection gas was injected through a 6-port valve using hydrogen as the carrier gas. A power supply was connected to the electrodes applying 100 V. A DLPCA-200 amplifier of FEMTO Messtechnik GmbH, Paul-Lincke-Ufer 34, D-10999 Berlin Germany was used for the evaluation for the micro-FID signal detection. The signal after the amplification was recorded with a U3-LV data requisition board of LabJack, Lakewood, CO, U.S.

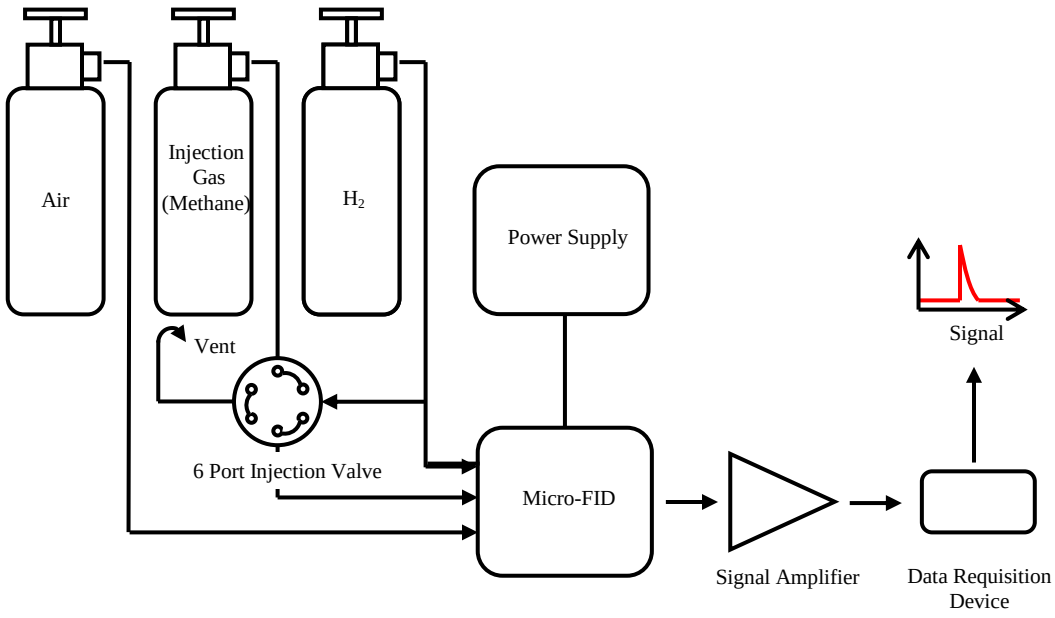

FIGURE 3. Schematic of the experimental setup, including the air, hydrogen, methane gas tanks, injection system, electrical power supply, and signal detection devices.

CHAPTER 3
FABRICATION

3.1 Silicon Channel Fabrication

In this section, a step-by-step description of the silicon channel fabrication is process is provided.

3.1.1. Patterning

1. Start with 750µm thick wafer.

2. Clean with Acetone and IPA and dry on 110C for 2min

3. Sputter front side of the wafer with Al for 25min (~1000A) or Cr for 9min (~1000A)

4. Spin coat topside of wafer with 4620 (PR), (3000rpm, 30sec).

5. Soft bake at 60°C for 2 min, and then at 110°C for 2 min. Protect wafer by aluminum ring.

6. Flip the wafer and repeat 4 – 5.

7. Cool the wafer on chuck for 30sec

8. Flip over the wafer then soft bake again at 110°C for 2 min. Protect wafer by aluminum ring.

9. Expose with first mask by using a contact Aligner (Top side alignment, about 20sec exposure).

10. Develop only two alignment marks by using dropping (pipette) AZ 400 K developer (4:1 of DI: developer) about 2min.

11. Check the developed alignment marks under the microscope.

12. Expose backside with a second mask by back-side alignment (about 20seconds exposure).

13. Develop wafer in AZ 400 K developer (4:1 and 10:1 of DI: developer) about 2min and 1min.

14. DI quench for 1min, N_2 dry.

15. Check the developed pattern by using microscope.

16. Al (Cr) etch in their etchant (Al etchant on 50°C hotplate) – 50% over etch (once the metal seems to be gone, count 50% more of the time that already past.

17. Rinse thoroughly in DI water, N_2 dry.

18. Check if all the metal is removed under microscope.

3.1.2. ICP-DRIE

1. Remove edge beads using acetone and swab.

2. Bake the wafer 135°C for 7min covered with Al foiled dish.

3. Ramp hot plate to 150°C, and begin timing when hotplate reaches 150°C for 15min.

4. Etch wafer in the ICP-DRIE using recipe "BOSCH-2" on the front side of the wafer at least half or more (about 1hours and 30 to 40min).

5. ICP-DRIE using recipe "BOSCH-2" on the back side of the wafer until you hear a alarm.

6. Repeat 20 loops and check if all the channels and holes are etched through, if not repeat another 20 loops; until all channels and holes are cleared

7. PR strip in 400T PR stripper on 120°C hotplate about 30min

8. Metal etching in Al (Cr) etchant – over etch 50%

9 DI quench 1min; DI cleaning thoroughly

3.1.3. Cleaning

1. Make the SC-1 solution (DI 200, Hydrogen Peroxide 20ml, Ammonium Hydroxide 2ml (or 58 drops)) and heat hotplate to 150°C

2. Transfer the wafer to SC-1 solution on hotplate

3. Set hotplate probe to 75°C; ramp & soak time 30 min

4. Transfer the wafer to DI / IPA glassware (100 /100 ml) 2 min

5. Rinse with IPA and completely dry

3.1.4. Grow thermal oxide layer for the electrical insulation layer

1. Make sure the O_2 is off and turn on N_2 from 2.5L/min to 6L/min.

2. Set the temperature of the oxidation furnace tube to 1100^{o}C.

3. Wait until the temperature is at least 900°C before loading the samples.

4. Load your samples if the tube furnace temperature is around 900^{o}C.

5. Take out the quartz boat with the clamp (leave the boat inside the tube), put your samples on the quartz boat, and place the quartz boat on the mouth of the tube. Wait about 2 minutes at the mouth of the furnace tube.

6. Push the boat in to the center of the tube very slowly.

7. Wait until the temperature reaches set temperature 1100^{o}C.

8. Change gas; Turn on O_2 flow to 6L/min; Then, Turn off N_2.

9. Start timing for 30 min.

10. Turn on N_2 to 6L/min. Then, turn off O_2

11. Set temperature to 400°C.

12. Wait until temperature reaches 900°C

13. Start to pull out your wafer out very slowly, unload your wafer and store the quartz plate and boat at the mouth of the tube.

14. Remove oxide in BOE. Rinse with IPA, and dry.

15. Repeat 2-8

16. Start timing over 12hours.

17. Repeat 10-13.

3.2. Electrode Fabrication

1. Start with a 25.4mm × 25.4mm × 1.5748mm quartz plate.

2. Spin AZ1518 with recipe #1 (@5000rpm)

3. Bake on 110C for 3min

4. Flood exposure 6 ~ 8sec

5. Develop in DI:AZ400K=4:1 for ~ 90sec (varying, need to be monitored on the fly)

6. DI quench for 1min

7. O_2 descum with 150W, O_2:Ar=2:1 for 1min

8. Sputter Cr for 1min.

9. Sputter Gold for 4min 15sec.

10. Photoresist lift-off using 1165PR stripper.

CHAPTER 4
RESULTS AND DISCUSSION

4.1. Flame visualization

Figure 4a shows a representative image of a flame taken with the ICCD camera. This flame structure is obtained when the air and hydrogen channel are at right angles to each other and the flow rates of air and hydrogen were 40 and 80ml/min. Two distinct flames one the left and right sides are observed. This flame structure can lead to loss of analytes, that is, analytes carried by the hydrogen stream can pass through the gap between the two distinct flames without being ionized. Thus this channel configuration leads to a loss of potential signal for the micro-FID. Figure 4b shows the flame shape obtained with the counter-flow channel design. In this design, air comes from the top flowing to the bottom while hydrogen comes from the bottom to the top with a flow rate of 80ml/min for both air and hydrogen. With this channel configuration a single narrow flame is obtained which has been tested in our previous experiments as a counter-flow flame.[8] However, the counter-flow flame design shown in Fig.4b has the potential for a loss of analytes out the two side exhaust channels. The tails of the flame allow the analytes to leak out the exhaust channels without being ionized, which also reduces the output amplitude.

When hydrogen and air channels meet with a 150° angle, a stable single flame is observed as shown in Fig. 4c. This flame structure is obtained by applying air with a flow rate of 80ml/min from the side and hydrogen with the flow rate of 80ml/min from the bottom. The advantage of this design is that a folded flame forms, which can confine the analytes in between the folded flame structure. This configuration increases the path length that the analyte travels

along, thereby increasing the average temperature of the injected analytes, which results in improving the ionization efficiency.

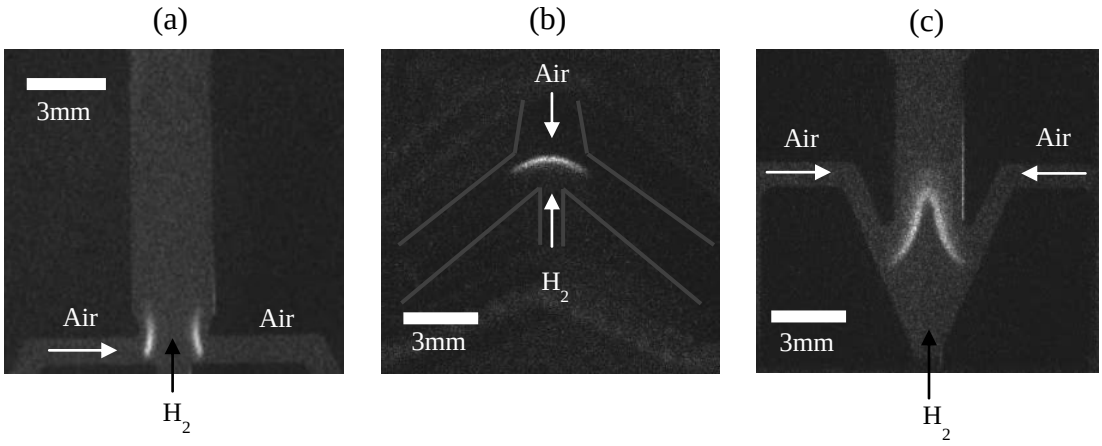

FIGURE 4. **(a)** A representative image of a flame taken with an ICCD camera. This flame structure is obtained when the air and hydrogen channel are at right angles to each other and the flow rates of air and hydrogen were 40 and 80ml/min.

(b) This flame structure is obtained with the counter-flow channel design. In this design, air is coming from the top flowing to the bottom while hydrogen is injected from the bottom to the top with a flow rate of 80ml/min.

(c) This flame structure is obtained by applying air with a total flow rate of 80ml/min from the side and hydrogen with the flow rate of 80ml/min from the bottom.

4.2. Signal Detection

First, we need to determine an optimal value of the voltage applied to the electrodes that will collect most of the generated ions. To do so, a flame was generated with the flow rate of 60ml/min and 175ml/min of hydrogen and air respectively. An amount of 0.045ml of methane with a pressure of 3atm (45psi) in room temperature was injected into the system, and the signal was observed while increasing the applied voltage. Figure 5 shows the amplitude of the injection

peak as the applied voltage varies. The amplitude steadily increases while the applied voltage increases up to 100 V, where the ionization reaches about its saturation point. Based on this result, it seems that 100 V is an amount of voltage that can collect most ions during the injection of the sample for the setup.

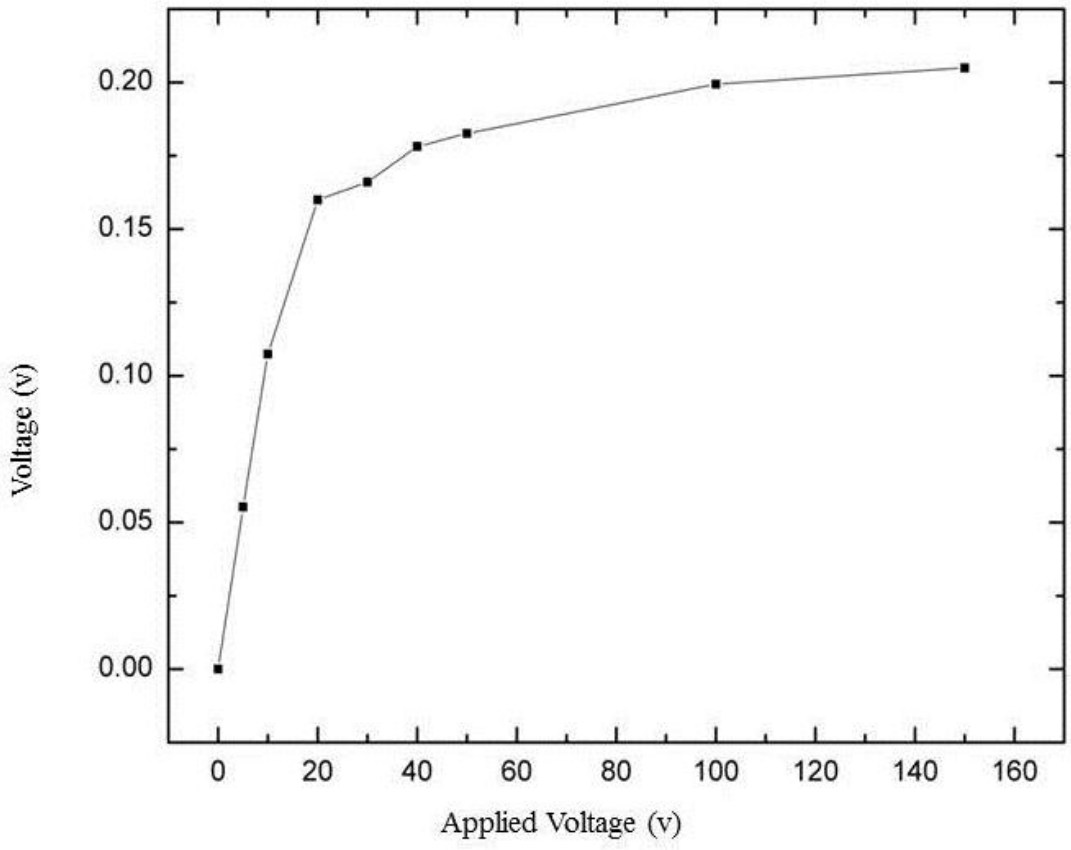

FIGURE 5. The plot shows the response signal in voltage of the injection peaks as the applied voltage is increased from 0 to 150V.

As shown in Fig.6, the electrode consists of two metal arms on each quartz plate. In order to obtain the highest signal, ten different configurations which are shown in Fig.6 were tested to evaluate the most suitable electrode configuration. In configuration #1 and #2, an electric field

parallel to the gas flow is applied, and in configuration #3 to #6, an electric field vertical to the gas flow was applied. In configuration #7 to #10, only one pair of the electrodes had a potential while the other pair is left to float. An amount of 0.045ml of methane gas with a pressure of 3atm (45psi) in room temperature was injected, and the response is measured with a picoammeter with an applied voltage of 100 V.

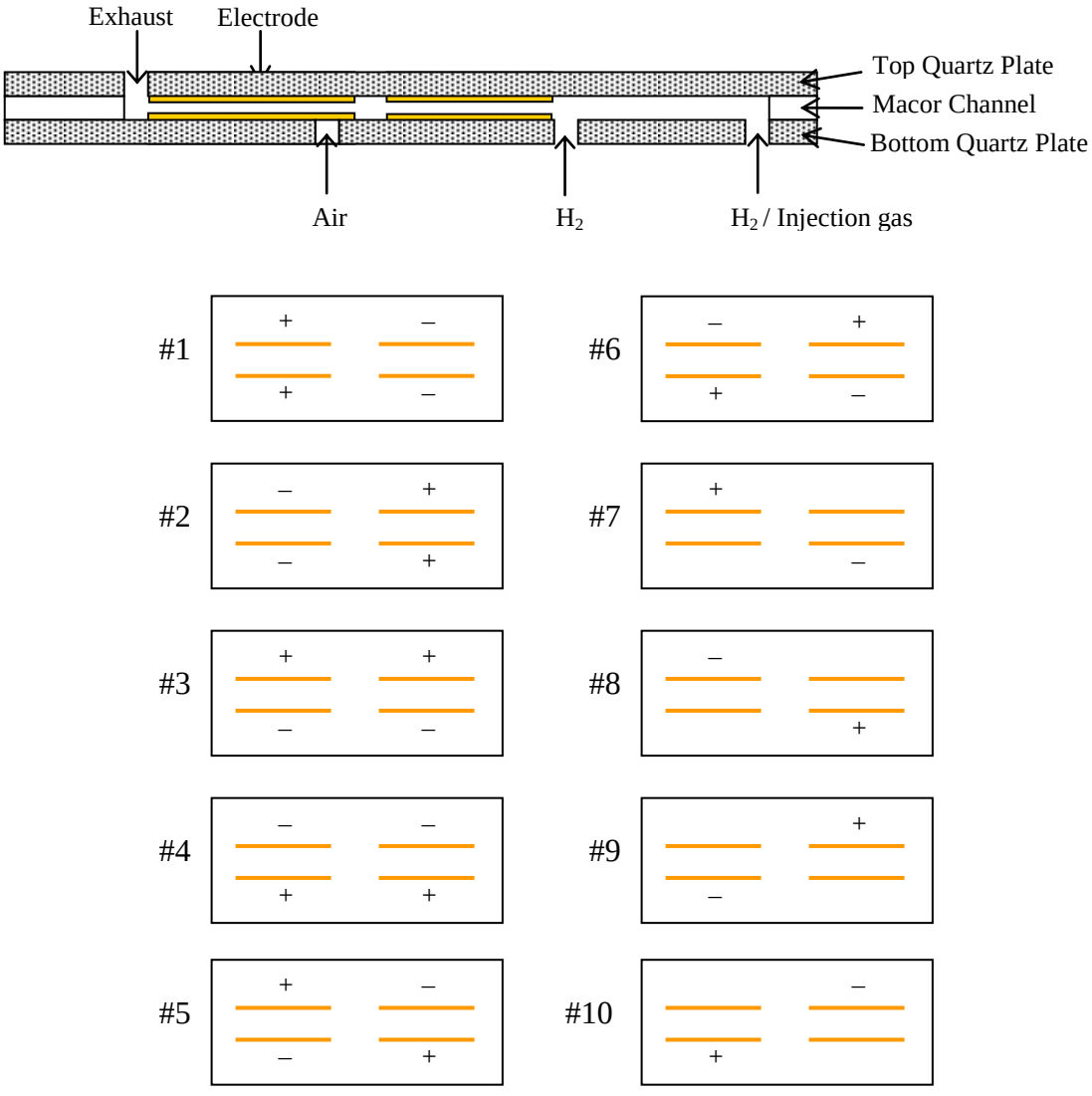

FIGURE 6. Tests for 10 different configurations of four electrodes have been performed to investigate the configuration that can generate the highest sensitivity.

The results in Fig.7 show that configurations #1 through #6 demonstrate about 30% higher sensitivity compared to the sensitivity obtained by configurations #7 through #10, in which one pair of the electrodes has a potential and the other pair is left to float. Based on the results shown in Fig.7, it an electric field created vertical to the gas flow collects about 5% more ions than the parallel electric fields. Configuration #3 was chosen for further experimentation.

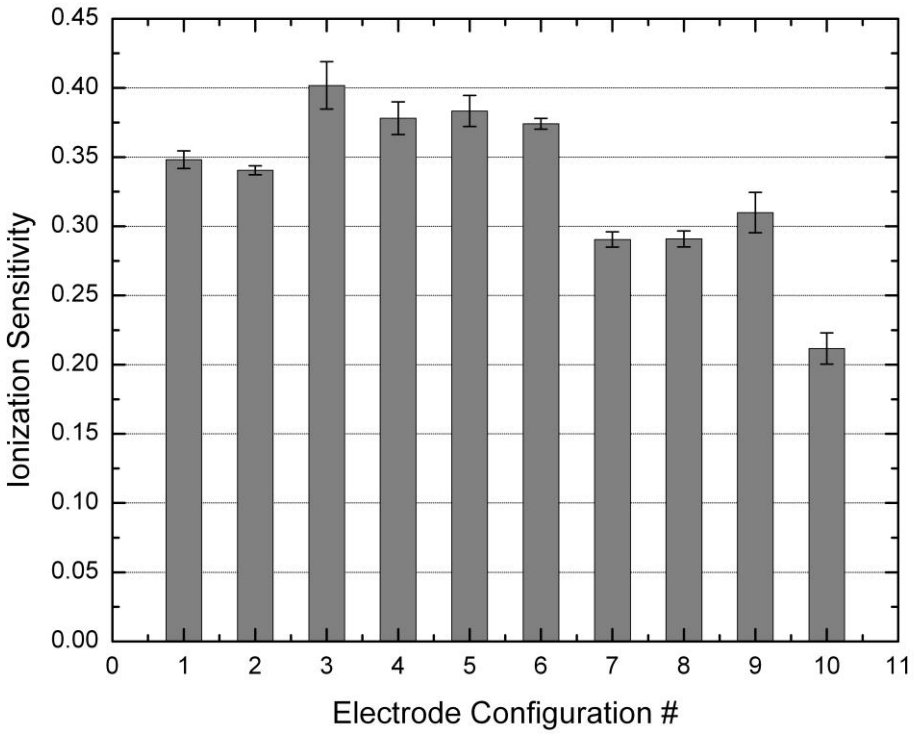

FIGURE 7. Signal detection using the 10 different configurations is shown.

4.2.1. Counter-flow Flame Design vs. Folded Flame Design

The channel designs were sandwiched together between two electrodes patterned on a quartz plate and tested. Figure 8 shows a typical response of the micro-FID over time when the folded flame and counter flame channel are used respectively. A methane sample gas of 0.045ml is injected and the flame is sustained with 120ml/min of air and 80ml/min of hydrogen. The picoammeter gain is set to 10^7 with 100V applied to the electrodes.

Testing in Fig. 8 is repeated four times, and the average area of the peak is shown in Table 1, which is about 0.0116V·sec and 0.3948V·sec for the counter-flow flame design and folded flame design respectively. Using the injection peak data, the ratio of the collected ions is calculated as follows. Injecting 0.045ml of methane results in 7.2×10^9 ions and 2.46×10^{11} ions collected for the counter flame design and folded flame design, respectively versus 1.21×10^{18} for total hydrocarbons in 0.045ml of methane gas. The collected electric charge per mole is chosen as a gauge of the ionization efficiency with a result of 1.959×10^{-2} C/mol. This is about 34 times higher compared to the result obtained using the counter-flow flame, which is 5.73×10^{-4} C/mol. This result shows that the folded flame structure enhances ionization with less leakage of the analytes compared to the counter-flow flame. Additionally, comparing these test results to the value of the ionization efficiency of a regular macro FID, which is 10^{-1} C/mol, shows that the ionization efficiency of the folded flame FID is within the range of 2 orders of magnitude of the macro FID's.[9]

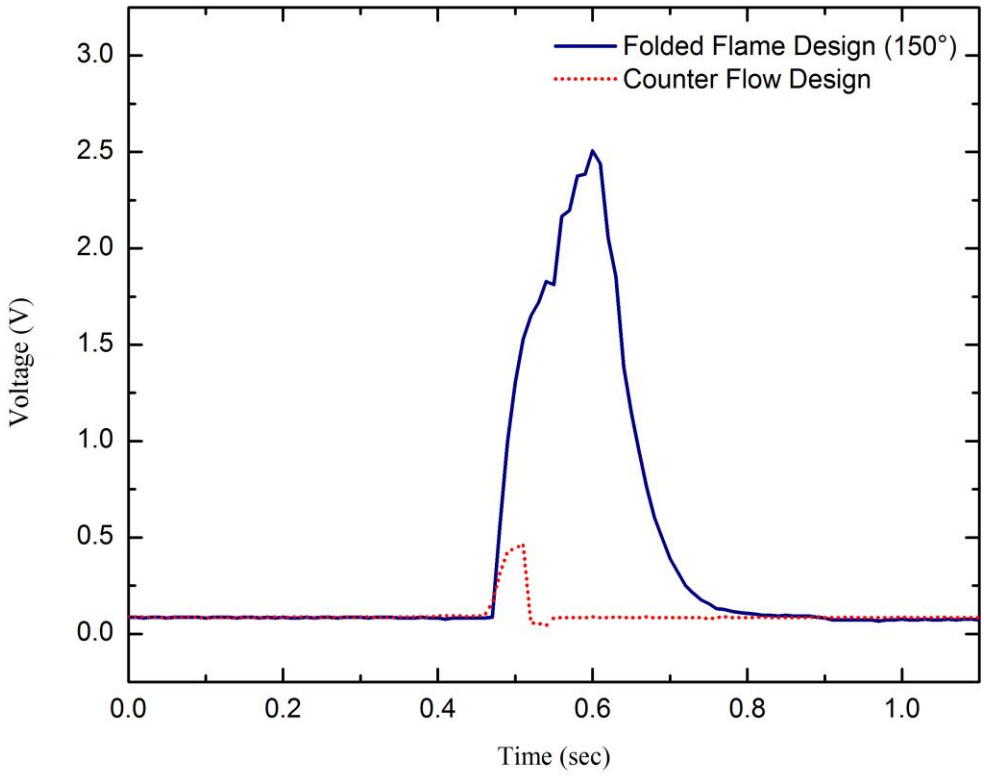

Figure 8. The plot shows two response signals that are overlaid for comparison purpose, one of which is from the folded flame design (solid) and the other is from the counter flow flame design (dot). These plots show the signal of the micro-FID over time when a sample gas of 0.045ml of methane gas is injected. The flame is sustained with 120ml/min of air and 80ml/min of hydrogen. The picoammeter gain is set to 10^7 with 100V applied to the electrodes.

	1st run Peak Area	2nd run Peak Area	3rd run Peak Area	4th run Peak Area	Average Peak Area
Counter Flow	0.0155299	0.0090763	0.0098353	0.0120112	0.0116132
Folded Flame Design (150°)	0.3929804	0.3976754	0.3989577	0.3897554	0.3948422

TABLE 1. Testing in Fig. 8 is repeated four times and each peak area is calculated and listed above. The average area of the peak is about 0.0116 and 0.3948 for the counter-flow flame design and folded

flame design respectively. This implies that for every 0.045ml of injected methane gas of 3atm (45psi) in room temperature, the peak area was about 34 times larger for the folded flame design.

4.2.2. More Test Results with the Folded Flame Design

The comparison between the counter-flow flame design and folded flame design showed that the folded flame design has a higher signal detection rate with the same fuel flow rate and injection amount.

More experiments were performed with the folded flame design. In order to achieve a better understanding between the fuel flow and the detection signals, various flow rates was used for the experiment. The experiment was performed by varying the flow rate of one of the gas flows while the other gas flow was fixed to a certain flow rate. The condition of the injection gas remained at 0.045ml of methane with a pressure of 45psi in room temperature. The picoammeter gain remained at 10^7 with 100V applied to the electrodes. Figures 9.1-9.3 display the voltage variation with time when the flow of hydrogen was fixed to 60ml/min, and air was increased from 80ml/min to 100ml/min. The increment of air with fixed hydrogen flow of 60ml/min, shows an increase in the voltage signal at this flow range.

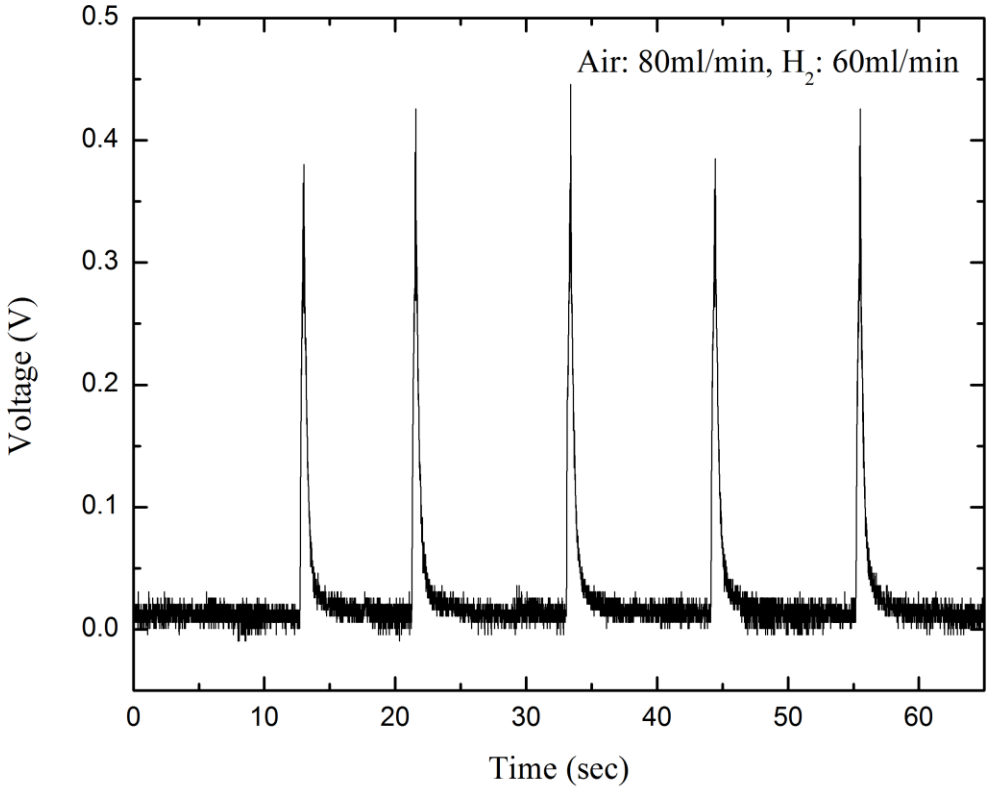

FIGURE 9. Air: 80ml/min, H_2: 60ml/min, injecting 0.045ml of methane with a pressure of 45psi in room temperature. Amplifier amplification is 10^7, and 100V of voltage is applied to the electrodes.

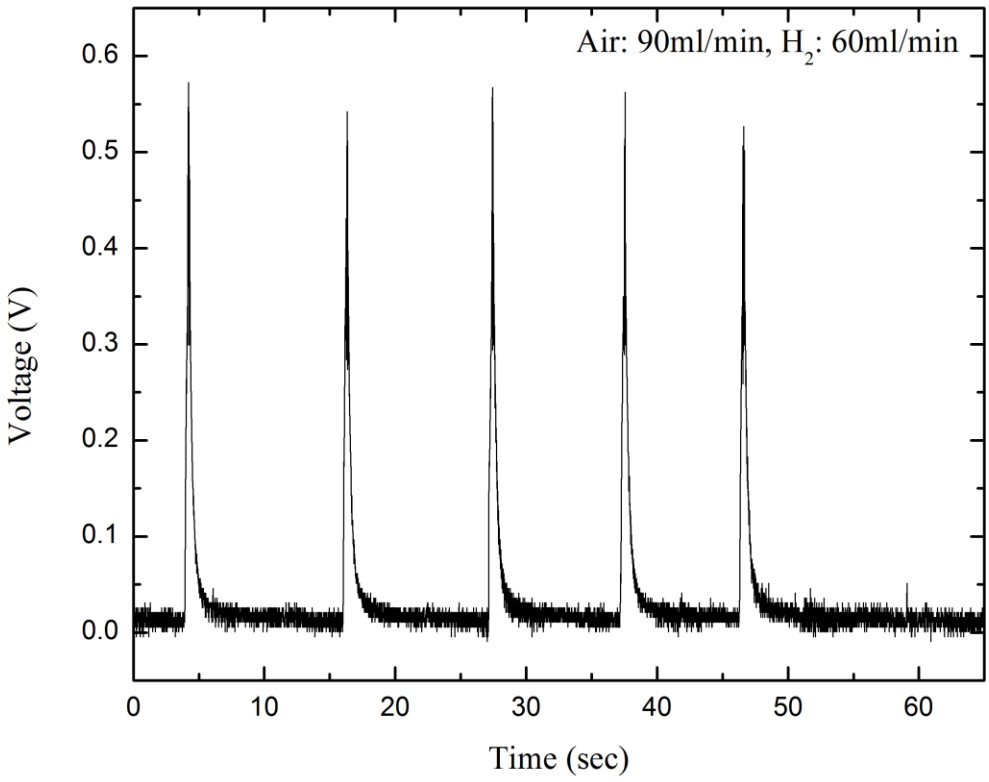

FIGURE 10. Air: 90ml/min, H_2: 60ml/min, injecting 0.045ml of methane with a pressure of 45psi in room temperature. Amplifier amplification is 10^7, and 100V of voltage is applied to the electrodes.

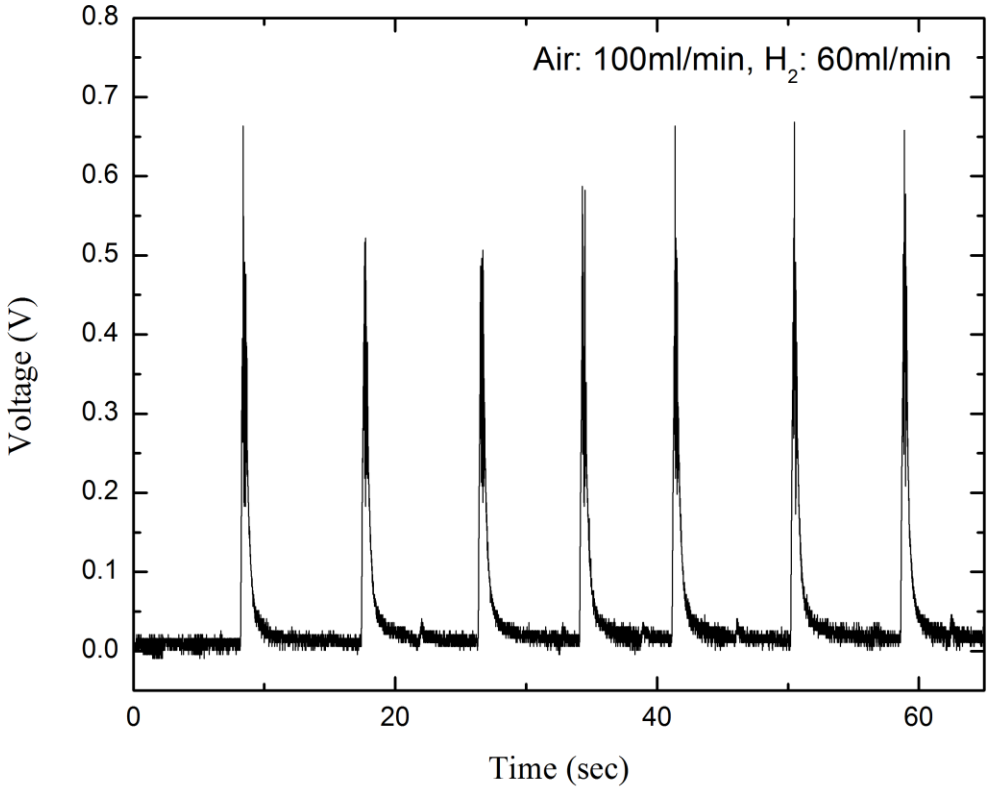

FIGURE 11. Air: 100ml/min, H_2: 60ml/min, injecting 0.045ml of methane with a pressure of 45psi in room temperature. Amplifier amplification is 10^7, and 100V of voltage is applied to the electrodes.

Figures 10.1-10.4 display recorded voltage when the flow of air is fixed to around 155ml/min, and hydrogen was increased from 25ml/min to 70ml/min. The increment of hydrogen with fixed air flow of 155ml/min, shows an increase in the voltage signal at this flow range.

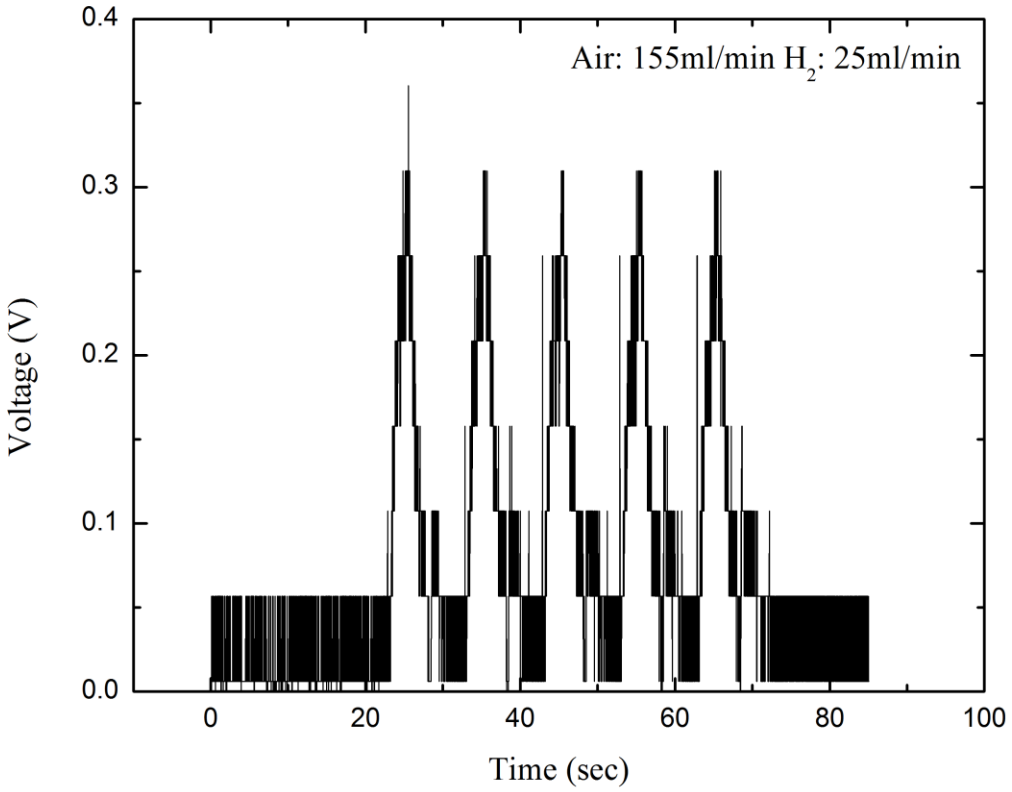

FIGURE 12. Air: 155ml/min, H_2: 25ml/min, injecting 0.045ml of methane with a pressure of 45psi in room temperature. Amplifier amplification is 10^7, and 100V of voltage is applied to the electrodes.

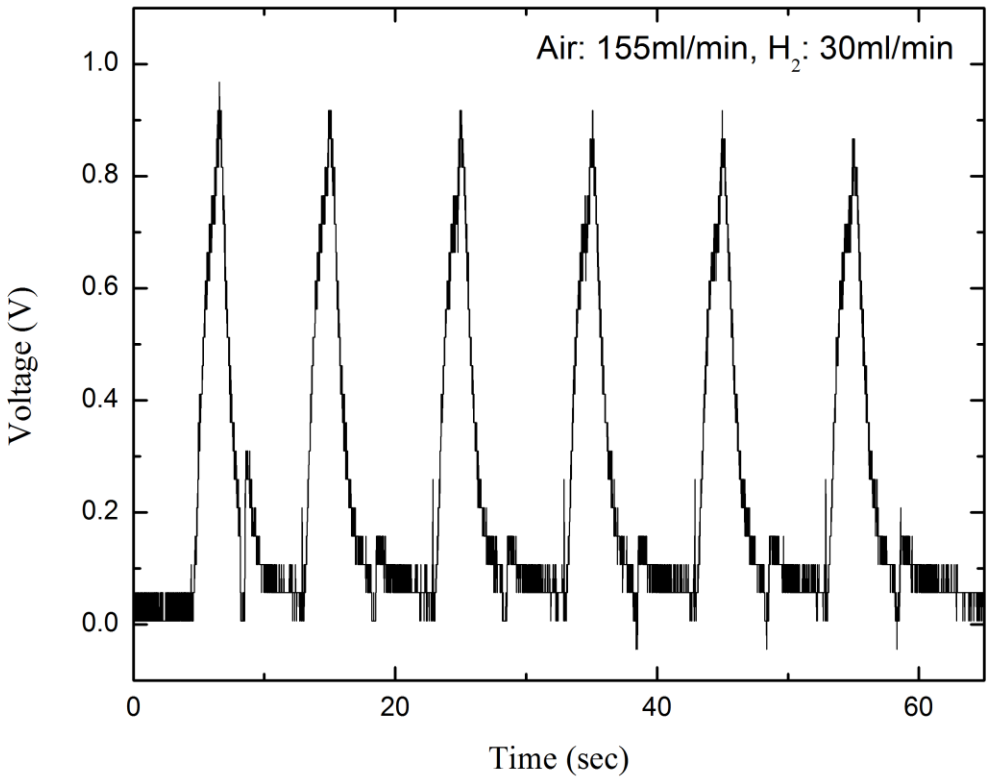

FIGURE 13. Air: 155ml/min, H_2: 30ml/min, injecting 0.045ml of methane with a pressure of 45psi in room temperature. Amplifier amplification is 10^7, and 100V of voltage is applied to the electrodes.

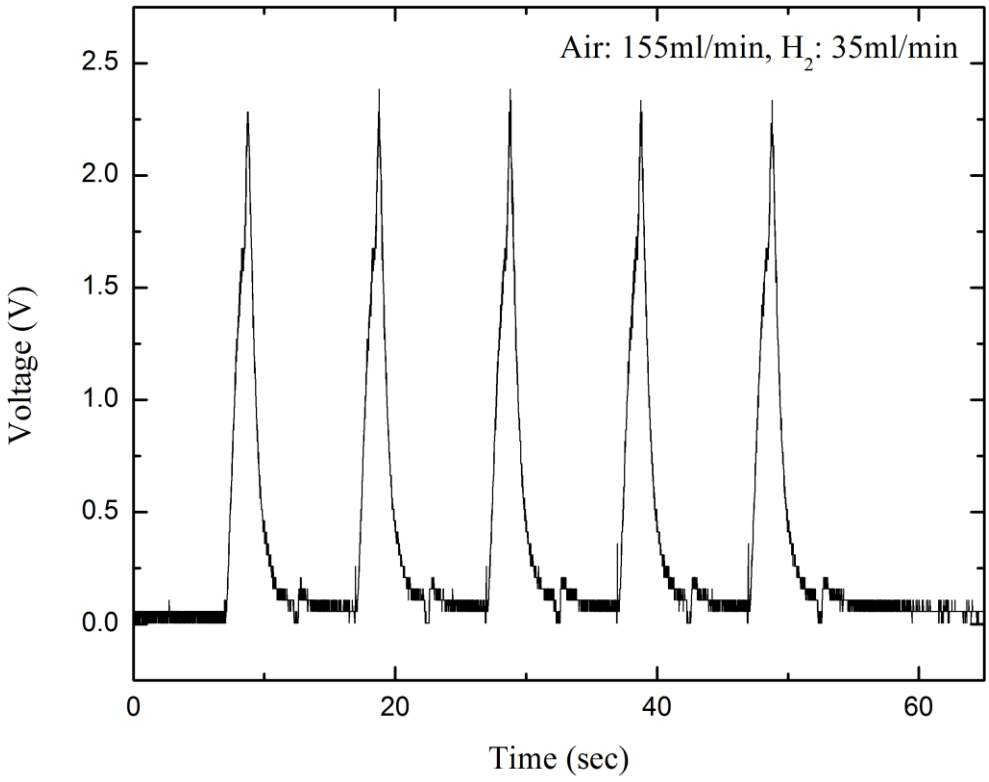

FIGURE 14. Air: 155ml/min, H_2: 35ml/min, injecting 0.045ml of methane with a pressure of 45psi in room temperature. Amplifier amplification is 10^7, and 100V of voltage is applied to the electrodes.

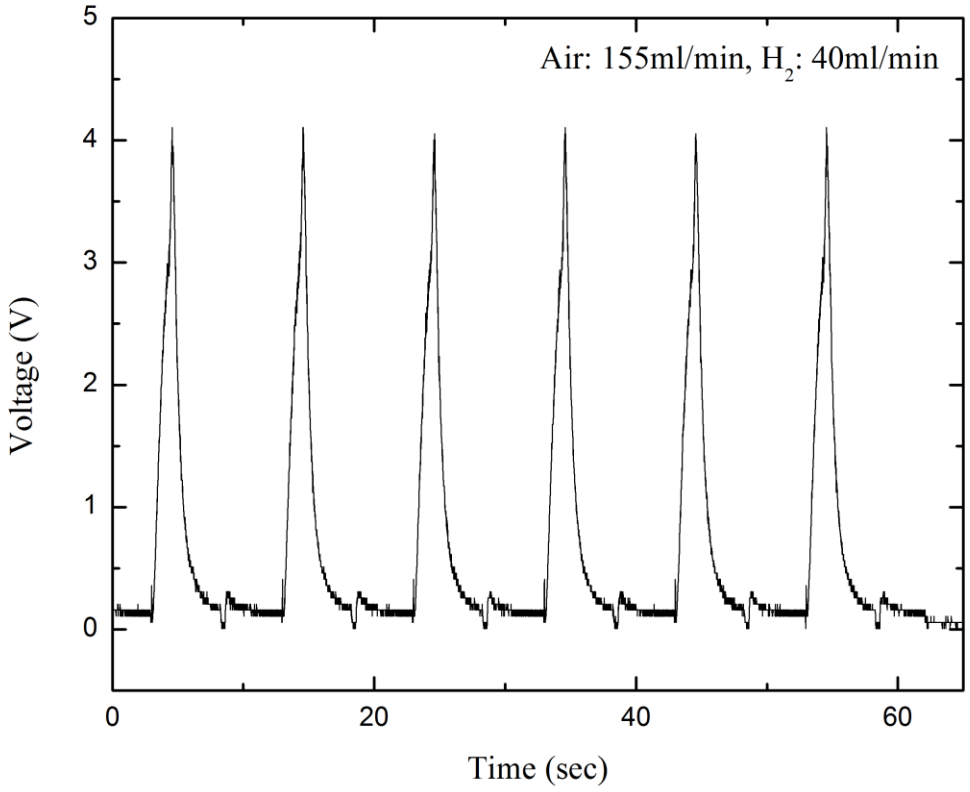

FIGURE 15. Air: 155ml/min, H_2: 40ml/min, injecting 0.045ml of methane with a pressure of 45psi in room temperature. Amplifier amplification is 10^7, and 100V of voltage is applied to the electrodes.

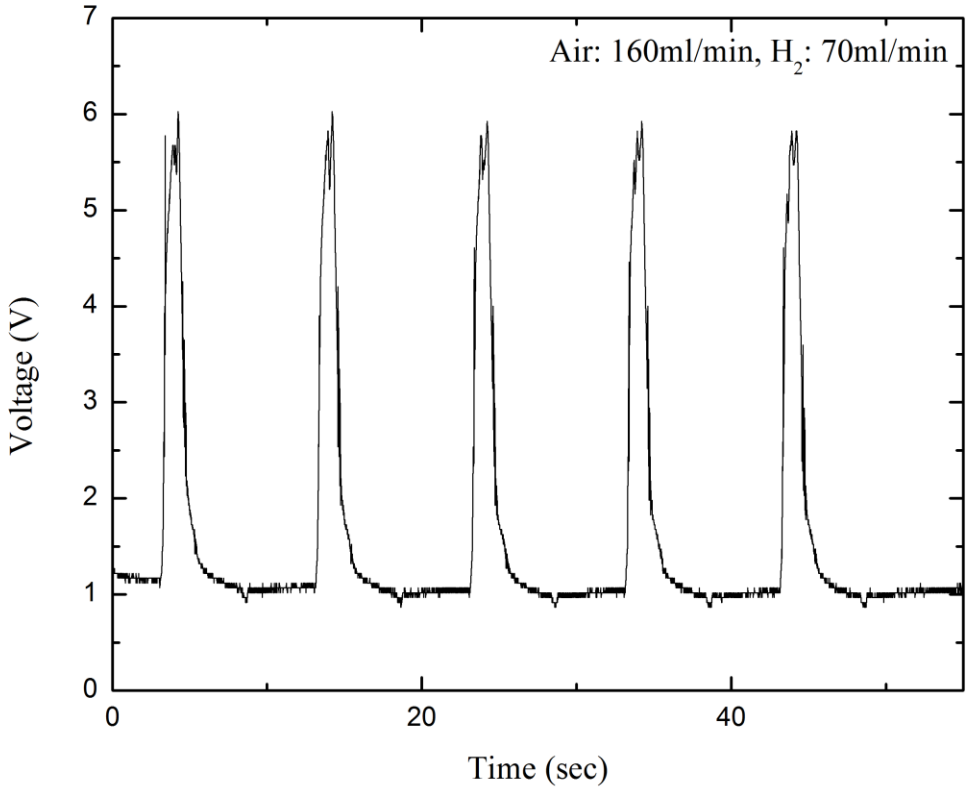

FIGURE 16. Air: 160ml/min, H_2: 70ml/min injecting 0.045ml of methane with a pressure of 45psi in room temperature. Amplifier amplification is 10^7, and 100V of voltage is applied to the electrodes.

CHAPTER 5

SUMMARY, CONCLUSIONS, AND FUTURE WORK

5.1 Conclusions and Summary

A stable diffusion flame with a folded shape was created by supplying air and hydrogen whose channels met with a 150° angle before creating the flame. The flame was sustained in a silicon or Macor structure with the threshold height of 750μm thickness. This folded flame structure confined the analytes in the flame, while increasing the pathway where the analyte travels, which increased the ionization efficiency. The electric charge per mole (C/mol) when injecting the methane sample was taken as a reference value to gauge the efficiency and the result was 1.959×10^{-2} C/mol which was about 34 times higher compared to the result obtained using the counter flow flame, which was 5.73×10^{-4} C/mol. The result showed that the folded flame structure enhanced more ionization with less leakage of the analytes compared to the counter flow flame.

5.2 Future Work

Several subjects have emerged as possible directions for the continuation of this research. Future work on the micro-FID should focus on further reduction of the flow rate. As portable analysis systems have become an increasing interest, the future work has to concentrate on the reduction in fuel consumption. The high fuel consumption rate for conventional FIDs makes

portability a challenge. The miniaturization of the FID will allow reducing fuel consumption for portable applications.

Increasing the signal-to-noise ratio to a level that can match commercial macro-scale FID's is needed. Current designs can be optimized by focusing on the improvement of the electrode designs and configurations. Using oxygen instead of air can increase the overall temperature of package, which can improve the ionization of the analytes.

More tests should be performed with different gas analytes. The current work described above is performed injecting methane only. Further experiment should be performed by injecting different types of hydrocarbons. The micro-FID will need to be connected to a GC, and a mixture of hydrocarbons can be injected to determine the signal response.

REFERENCES

[1] C. Washburn, M. W. Moorman, T. W. Hamilton, A. L. Robinson, C. Mowry, R. G. Manley, G. Shelmidine and R. P. Manginell, "Micro-flame ionization detection using a catalytic micro-combustor," in *Proceedings of IEEE Sensors*, 2005, pp. 322-325.

[2] T. C. Hayward and K. B. Thurbide, "Carbon response characteristics of a micro-flame ionization detector," *Talanta*, vol. 73, pp. 583-588, 9/30, 2007.

[3] T. C. Hayward and K. B. Thurbide, "Novel on-column and inverted operating modes of a microcounter-current flame ionization detector," *Journal of Chromatography A*, vol. 1200, pp. 2-7, 7/18, 2008.

[4] M. Moorman, R. P. Manginell, C. Colburn, D. Mowery-Evans, P. G. Clem, N. Bell and L. F. Anderson, "Microcombustor array and micro-flame ionization detector for hydrocarbon detection," in *Proceedings of SPIE - the International Society for Optical Engineering*, 2003, pp. 40-50.

[5] W. J. Kuipers and J. Müller, "A planar micro-flame ionization detector with an integrated guard electrode," *J Micromech Microengineering*, vol. 18, 2008.

[6] S. Zimmermann, S. Wischhusen and J. Müller, "Micro flame ionization detector and micro flame spectrometer," *Sensors and Actuators, B: Chemical*, vol. 63, pp. 159-166, 2000.

[7] S. Zimmermann, P. Krippner, A. Vogel and J. Müller, "Miniaturized flame ionization detector for gas chromatography," *Sensors and Actuators, B: Chemical*, vol. 83, pp. 285-289, 2002.

[8] T. Kang, J. Kim, B. Bae and M. A. Shannon, A Micro-burner Based Flame Ionization Detector for Micro-scale Gas Chromatographs, *Proceedings of the 6th U.S. National Combustion Meeting* (Ann Arbor Michigan, 2009), 13A2

[9] J. Sevcik, "Detectors in gas chromatography," *Journal of Chromatography Library*, vol. A, pp. 94-95, 1975.